

# Do Single Matrix Molecules Generate Primary Ions in Ultraviolet Matrix-assisted Laser Desorption/Ionization?

Volker Karbach and Richard Knochenmuss\*

Laboratorium für Organische Chemie, Universitätsstr. 16, ETH Zürich, CH-8092 Zürich,  
Switzerland

Published as:

*Rapid Commun. Mass Spectrom.* **12**, 968–974 (1998)

DOI: 10.1002/(SICI)1097-0231(19980731)12:14<968::AID-RCM255>3.0.CO;2-4

## Abstract

The ionization mechanisms in matrix-assisted laser desorption/ionization (MALDI) remain poorly understood. We have begun a program of study aimed at determining the properties of matrix molecules which make them suitable for MALDI. Initial results are presented here for one of the most widely used matrix materials, 2,5-dihydroxybenzoic acid (DHB). Spectroscopy of free DHB molecules in a molecular beam shows that the photoionization energy is much lower than expected from semiempirical calculations, only 8.05 eV, yet still not accessible with two nitrogen laser photons (7.36 eV). No evidence is found for labile protons in the first excited state. This is in spite of structural similarity with salicylates where excited state proton transfer from the 2-hydroxy group occurs. Conventional excited state proton transfer from single DHB molecules to analytes is thus deemed unlikely. On the other hand, a two-step reaction taking place via decarboxylated DHB (hydroquinone) is shown to be a potential analyte protonation mechanism. The conclusion is reached that single matrix molecules are probably not the primary ion generators in UV MALDI with this matrix. This is consistent with proposed models which require dimers or larger aggregates for ion generation. The photo/thermal combined ionization model of Allwood, Dyer and Dreyfus (*Rapid Commun. Mass Spectrom.* 11, 499 (1997)) is updated with measured physical parameters for DHB, and extended to include 2-center energy pooling mechanisms.

## Introduction

The photophysical and photochemical properties which make some materials suitable as MALDI matrices remain largely unknown, as do MALDI ionization mechanisms in general. Numerous ionization mechanisms have been proposed<sup>1-4</sup>, many proceeding via single matrix molecules which are excited by one or two laser photons into a reactive state. For positive ions, the first possibility that comes to mind, and that most frequently proposed, is simple two-photon ionization of the matrix, followed by subsequent reactions with the analyte or other matrix molecules. On the other hand, many analytes are observed in MALDI primarily as the protonated adduct, leading one to consider excited state proton transfer reactions from a non-ionized, singly excited matrix to the analyte.<sup>3,4</sup> This has led to the proposal that *ortho*-hydroxy aromatic acids (such as 2,5-dihydroxybenzoic acid (DHB)) are generally good matrices due to the potential for intramolecular excited state proton transfer from the hydroxyl to the acid carbonyl.<sup>5</sup> Such intramolecular reactions have been known since the early measurements on methyl salicylate in solution by Weller.<sup>6</sup> Presumably the labile proton could also be donated to an analyte that might be hydrogen bonded at the correct position, rather than to the carbonyl.

Using only a mass spectrometer, definite identification of a particular ionization pathway from the final products is quite difficult. In contrast, direct measurement of certain matrix properties can rapidly establish whether a given pathway is possible or not. For example, knowledge of the ionization potential (IP) allows a simple calculation to determine the number of 337 nm nitrogen laser photons that are needed to ionize the molecule. We report here on this and other properties of DHB, which is one of the most popular MALDI matrices today. We find that single DHB molecules are probably *not* the primary ion generators in MALDI when using this matrix.

## Experimental

Free, cold DHB was generated in a molecular beam apparatus which has been recently described.<sup>7</sup> A brief description follows: solid DHB (Fluka) was placed into a pulsed nozzle, and heated to 150°C to generate a few mbar of vapor pressure. Neon gas at 1.1 bar passed over the DHB and the resulting mixture was expanded into a vacuum of typically  $2 \times 10^{-5}$  mbar. Clusters were generated by passing the carrier gas through a bubbler filled with the desired liquid material, typically held at 0°C in an ice bath. This mixture then was fed into the pulsed nozzle as for the other experiments.

For dispersed fluorescence measurements, the emitted light was collected at 90° to both the flow and laser axes, and dispersed with a 0.5 m,  $f = 4$  monochromator (SPEX 500M, 2400 l/mm grating), and detected with a photo-multiplier (Hamamatsu R3896).

For two-color, two-photon ionization experiments, Nd:YAG pumped dye lasers were used (Lambda Physik FL 2002 and modified FL 2001). The dyes used were pyridine 1, pyridine 2 and fluorescein 27. After doubling in KDP crystals, the UV pulse energies were 30–70 mJ in about 5 ns. Nominal pulse irradiances are reported here assuming a square 5 ns pulse. This is a substantial underestimate, since these dye lasers emit at a number of closely spaced frequencies simultaneously, leading to so-called mode beating and strong temporal structure in the pulse. Spikes of about 200 ps width are typical inside the nanosecond envelope.<sup>8</sup> Our nominal irradiances are therefore believed to be at least an order of magnitude lower than the true peak powers in the pulses.

The laser beams were crossed in the acceleration region of a linear 1 m time-of flight (TOF) mass spectrometer, downstream of a 1.5 mm skimmer. The pressure in the TOF region was  $2 \times 10^{-7}$  mbar. The resulting ions were accelerated to 5 keV and detected by a MicroSphere plate (El Mul Technologies). The solution spectra ( $10^{-5}$  M DHB in water) were taken on a Perkin Elmer LS-50 spectrometer.

## Results

### Absorption spectra

Two-pulse experiments have recently been reported which show that the lowest excited state of DHB is the gateway to UV-MALDI ionization.<sup>9,10</sup> Two time-delayed subthreshold pulses incident on a MALDI sample lead to strong signals, for delays up to 10 ns. Either these excited molecules react, possibly by proton transfer, or they store energy and are then further excited and ionized. Interestingly, the two-pulse optimum pulse delay is close to the solid phase fluorescence lifetime of 5 ns,<sup>11</sup> suggesting that energy storage is more likely. In either case the study of DHB MALDI ionization must begin with the molecular absorption spectrum.

In Fig. 1 is shown the fluorescence-detected absorption spectrum of expansion cooled DHB molecules in the vacuum. Detection was via total fluorescence, i.e. not wavelength selective. All emitting species are therefore detected, including, for example, dimers or other clusters, which lead to weak bands near the baseline. The strong peaks are all due to DHB monomer, as was verified by mass-selective two-photon ionization spectroscopy. Each of the 3 hydroxyl groups can have one of two orientations with respect to the other substituents, leading to at least eight possible conformers of the molecule. The conformation shown was calculated by ab initio methods to be the lowest in energy, and we presume this to be the dominant species observed.

The electronic origin transition for this conformer is found at  $27\,957\text{ cm}^{-1}$  (357.69 nm). The spectrum is quite congested, there are numerous Franck–Condon active modes which form progressions and combinations. These lead to a nearly continuous absorption at energies of more than about  $1200\text{ cm}^{-1}$  above the origin. The nitrogen laser ( $29\,674\text{ cm}^{-1}$ ) is capable of directly exciting free DHB, and thereby deposits about  $1700\text{ cm}^{-1}$  of excess energy in the first excited singlet state ( $S_1$ ).

### Two-photon ionization and ionization potential

In the most frequently considered ionization mechanism, a second photon is presumed to be absorbed by excited DHB, leading to ionization. If we use one laser to excite at the frequency of one of the bands in Fig. 1 we can create a significant population of molecules in the  $S_1$ . A second laser is then used to ionize these molecules. This laser is scanned to

obtain a photoionization efficiency curve, as a function of the total two photon energy. As shown in Fig. 2 DHB is first ionized by this process at a total energy of  $27\,957 + 36\,950 = 64\,907\text{ cm}^{-1}$  or 8.05 eV. (Correcting for the 144 V/cm acceleration field of the mass spectrometer gives a field-free value  $72\text{ cm}^{-1}$  higher.) This is substantially above twice the nitrogen laser photon energy of  $2 \times 3.68 = 7.36\text{ eV}$ . The pulse energy of the second, ionizing laser was varied from the minimum needed to see any ions ( $<5\text{ }\mu\text{J}$ ) to the maximum available ( $35\text{ }\mu\text{J}$ ). Plotting the ion signal against the pulse energy gave a good linear dependence, showing that the  $S_1$  to ion step is a single photon process. The two-color experiment is then a  $1+1'$  two-photon ionization.

Below the ionization potential (IP) step of Fig. 2 the ion signal is very small. At an ionization wavelength of 280 nm, or only  $1235\text{ cm}^{-1}$  below the IP, we were unable to detect any DHB ions at  $10^6\text{ W/cm}^2$  (ionization laser), at a noise-limited sensitivity of about 0.2% of the signal above the IP. (Nearer the IP there are weak DHB signals from fragmenting dimers.) In an attempt to induce one-color 3-photon ionization via the electronic origin, the ionizing laser was blocked, and the exciting laser focused in the vacuum chamber. At a nominal irradiance of  $3 \times 10^7\text{ W/cm}^2$ , a signal of 0.3% of the two color value was obtained. Corrected for the smaller sampled volume, this corresponds to 5% of the two color intensity, but is close to our detection limit. As noted above, the true peak irradiances were almost certainly an order of magnitude higher, or above  $10^8\text{ W/cm}^2$ .

### Fluorescence Spectra

An excited-state proton transfer (ESPT) reaction is best detected by fluorescence spectroscopy. After excitation, reaction causes rearrangement of the electron distribution in the molecule, which must be reflected in the subsequent emission spectrum. In particular, the fluorescence will lose any semblance of mirror symmetry with the absorption spectrum, and a dramatic shift to lower energy is typical.

In Fig. 3(a) we show the dispersed fluorescence spectrum after excitation of DHB at the electronic origin of the  $S_1$  state. The emission begins at the same wavelength as the excitation, there is no anomalous red shift. Further, the sharp line structure can be assigned as vibrations with well-defined counterparts in the absorption spectrum. (At higher resolution each band in the Figure is found to be composed of several peaks.) As in

absorption there are many active modes, so the spectrum is congested. A detailed analysis shows that for most active modes the strongest fluorescence transitions are those for which the vibrational quantum number increases by 1. The maximum in the emission should thus occur at the wavelength where all these vibrations make a  $\Delta v = 1$  transition, in this case at an estimated shift of  $1850\text{ cm}^{-1}$  from the electronic origin. The observed maximum is at a shift of  $2100\text{ cm}^{-1}$ , in satisfactory agreement.

The similarity between the free molecule fluorescence and that in water solution is shown in Fig. 3(b). The gas-phase spectrum has been shifted laterally to compensate for solvation. As is apparent, solvation does not induce extra broadening.

#### DHB decomposition and photoionization of mixed clusters

In addition to DHB, it is typical that a certain amount of hydroquinone (HQ, or 1,4-dihydroxybenzene) is observed in the supersonic expansion. This is formed by thermal decomposition of DHB inside the nozzle, as can be checked by changing the nozzle temperature. HQ can be ionized in a one-color 1+1 process with laser wavelengths in the range used for ionization of DHB. The identity of the  $m/z$  110 peak was also verified as due to hydroquinone by comparison with literature spectra, and by loading HQ into the nozzle.

When triethylamine (TEA) is introduced into the gas stream of the apparatus, DHB signals decrease, leaving only HQ and its clusters with TEA, as shown in Fig. 4. From the residue found afterward in the nozzle, TEA appears to react with DHB vapor before expansion into the vacuum, explaining the loss of that signal. At the same time, one observes a 2-photon ionization signal at  $m/z$  102, corresponding to  $\text{TEA}\bullet\text{H}^+$ . By changing the laser wavelength or the expansion conditions, this signal was found to be correlated with  $m/z$  211, or  $\text{HQ}\bullet\text{TEA}^+$ . The  $m/z$  102 peak also shows a distinct tail to higher mass, as is typical for fragment ions.

## Discussion

### Single molecule vs. solid phase absorption spectra

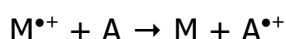
As seen in Fig. 3(b) the first absorption band of DHB in water solution peaks near  $31\,250\text{ cm}^{-1}$  (320 nm), dropping to 10% intensity at about  $28\,150\text{ cm}^{-1}$  (355 nm) on the long wavelength side. The absorption in methanol is similar. The single crystal spectrum extends to much longer wavelengths, with a steep edge at about  $26\,300\text{ cm}^{-1}$  (380 nm).<sup>3</sup> Prepared as solid films, variable results have been obtained. Heise and Yeung<sup>12</sup> found a main absorption band at about  $28\,150\text{ cm}^{-1}$  (355 nm), with a long tail extending to at least  $20\,000\text{ cm}^{-1}$  (500 nm). Allwood *et al.*<sup>13</sup> found a broader main absorption feature extending from about  $30\,000$  to  $26\,000\text{ cm}^{-1}$  (330 to 380 nm), but also observed weaker absorption to near  $20\,000\text{ cm}^{-1}$ .

The shift of intensity to lower photon energy in the solid phase can be attributed to intermolecular interactions, which delocalize the excitation onto more than one center. The main absorption, however, remains sufficiently similar to the dilute solution spectrum that it can be considered nearly localized on a single DHB molecule. The usual MALDI nitrogen laser operating at 337 nm ( $=29\,674\text{ cm}^{-1}$  or 3.68 eV) thus excites solid DHB into a largely localized, single molecule state, with properties that should be very similar to the free molecules studied here.

### Ionization potential and electron transfer reactions

The measured IP of DHB (8.05 eV) is much lower than that calculated by the MOPAC/PM3 method,<sup>14</sup> where a value of 9.04 eV was found. With the semiempirical basis sets contained in the GAMESS package<sup>15</sup> we have also obtained (Koopman) IP values in the range of 9 eV: 8.97 (PM3 basis), 9.04 (AM1) and 8.79 (MNDO). Hartree-Fock ab initio methods are somewhat better. A value of 8.54 eV is obtained after geometry optimization at the 4-31G level, but this is still substantially above the experimental IP.

The low IP may explain the rarity of analyte radical cations in MALDI. Such ions could be created by electron transfer reactions with ionized matrix:



where M = matrix and A = analyte. The DHB radical cation is observed strongly in MALDI mass spectra, but only infrequently are analyte radical cations found. This reaction is favorable only if the matrix IP is higher than that of the analyte. Since DHB has an unusually low IP for a molecule of its size, the reaction is unfavorable for many analytes. In particular, free amino acids all have higher IPs than DHB, with the exception of tryptophan at 7.5 eV.<sup>16</sup>

#### Fluorescence spectra and excited state proton transfer

In salicylates where ESPT is believed to occur,<sup>17</sup> a diagnostic strong fluorescence band is observed, peaking near 22 000 cm<sup>-1</sup>(450 nm) for the free molecule. This is clearly not found in Fig. 3(a), despite the low energy tail. The overall form of the spectrum is instead very similar to that of the closely related 5-methoxy salicylic acid, where no intramolecular ESPT was found.<sup>18</sup> Considering the fluorescence spectra in more detail, salicylic acid shows the behavior expected if ESPT occurs. The vibrational structure is very complex, and bears little resemblance to the absorption spectrum.<sup>17</sup> In contrast, the DHB spectrum, while congested, can be readily assigned and is consistent with the absorption spectrum.

Although the free DHB molecule shows no fluorescence which can be ascribed to intramolecular ESPT, this alone does not rule out intermolecular reactions. Clearly, however, the 2-hydroxyl proton is not as labile as in some related molecules. The environment can play a strongly stabilizing role in ESPT reactions,<sup>19</sup> making an otherwise unfavorable reaction possible. This is because of the charge separation in such reactions, and the ability of polar neighbors to reorient and stabilize the products. We tested the possibility that such assistance would induce ESPT in DHB by generating clusters of DHB with up to about 10 water molecules. Water is often the best such solvation partner, due to its mobility, polarity and hydrogen bonding ability. Only a minimal red shift in the maximum of the fluorescence spectrum was observed, giving no indication of an induced ESPT reaction.

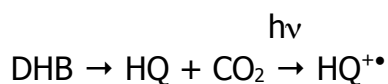
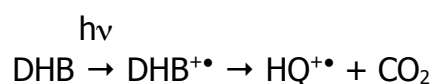
This is also consistent with the water solution results shown in Fig. 3(b). The absorption/emission symmetry is good, and there is no excessive gap between the two, such as that seen for salicylic acid.<sup>6</sup> In addition, the position and shape of the fluorescence band were not found to have a strong solvent dependence. In water the emission peak is



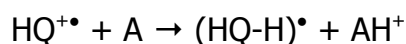
at 22 500 cm<sup>-1</sup>, in methanol at 22 350, in tetrahydrofuran at 22 900 and in dimethylsulfoxide at 23 150 cm<sup>-1</sup>. In all cases the width was between 3500 and 4000 cm<sup>-1</sup>. The relatively small differences between strong hydrogen bonding and proton accepting solvents like water and the much less active tetrahydrofuran and dimethylsulfoxide can be explained by non-specific dipole and polarization interactions. We conclude that neither intra- nor intermolecular ESPT are induced by these solvent environments.

Protonated analyte is strongly observed in MALDI, and has also been observed under some conditions as a product of photoexcited DHB/analyte clusters.<sup>20</sup> Therefore some type of proton transfer reaction does take place. Detailed analysis of the free molecule spectra suggest that a significant excited state distortion occurs, but without major charge separation. ESPT may be induced under special conditions, such as in a DHB dimer, and studies of this and other possibilities are under way. Our results show, however, that the simple single molecule ESPT explanation for MALDI protonation is probably not correct.

An example of the alternative proton transfer processes that may be active in MALDI is suggested by the results of Fig. 4. The HQ•TEA<sup>+</sup> cluster ion breaks into asymmetric fragments, abstracting a proton from HQ in the process. We thus obtain a protonated 'analyte' signal in our mass spectrum. A two step MALDI analyte protonation process can then be proposed for DHB matrix. HQ is first created from either neutral or ionized DHB (specific photoionization mechanisms are discussed in more detail below):



Next, ionized HQ encounters (or is near) an analyte, and a proton is transferred:



Although *m/z* 110 (HQ) is not normally observed in DHB MALDI spectra, we have found that HQ is indeed produced. Knowing the absorption spectrum as measured in the molecular beam, we were able to selectively ionize HQ in a DHB desorption plume,

thereby generating  $m/z$  110 in the mass spectrum. The extent to which the above protonation pathway actually leads to analyte signal in MALDI is not yet established, but it must now be considered a plausible contributor.

### Three-photon ionization

The results presented here show that sequential two-photon ionization of DHB with a nitrogen laser is not possible. A minimum of three such photons are required for this process. Although MALDI signal (desorption plus ionization) has been found to have a high order fluence dependence,<sup>21</sup> this is not an indication that direct multiphoton ionization is operative, since MALDI is a composite of both desorption and ionization. More concretely, our attempts to observe absorption of two photons from the  $S_1$  to generate ions (i.e a net 3 photon process) yielded very little signal, even at high irradiances. On the other hand, a small number of ions were generated in this manner, so 3-photon ionization of DHB under normal MALDI conditions cannot be completely excluded. As discussed below, however, two-photon plus thermal excitation is probably much more efficient.

In this context it is important to note that we have discussed irradiance or power density rather than fluence or energy density. This is because a high irradiance pulse is able to induce multiphoton processes of all kinds. High fluences are only relevant under special conditions which are limiting cases of high irradiance processes. In particular, multistep mechanisms with long-lived intermediate states (vs. the laser pulse width) will depend more on the number of photons delivered than on the rate of delivery. This appears to be the case in UV MALDI with DHB, as indicated by time-delayed 2-pulse experiments.<sup>9,10</sup> Ion signal is dependent on fluence rather than irradiance, under typical conditions. (Although this is partly a result of the fact that desorption must be induced, as well as ionization, and requires substantial heating of the sample.)

The fluence dependence of MALDI is also an argument against 3-photon ionization of single DHB molecules. Excitation to the  $S_1$  is efficient, so a 3-photon signal will be kinetically limited by the second step, two-photon absorption to the ion state. If this does not involve an intermediate state, the signal will be dependent on the square of the irradiance, not fluence. If it proceeds by two steps and a resonant intermediate state, then the rates of excitation and relaxation become important. Since relaxation from higher

excited states is almost universally very rapid (picoseconds) in condensed phase at or above room temperature, excitation must be quite fast to compete. In other words, irradiance rather than fluence is again the relevant parameter. If, on the other hand, ionization requires only one photon, the rate at which these photons are delivered is not important, if the intermediate state is long lived on the laser timescale, as observed.

#### The single and two-center two-photon plus thermal models

Although we conclude that a three-photon ionization mechanism is not supported by the data, a variant of the two photon ionization process remains to be considered. Allwood *et al.*<sup>22</sup> have suggested that two-photon excited matrix molecules may be ionized if the desorbing material is hot enough to compensate for the energy defect to the ion state. Others have also modeled MALDI desorption and ionization via thermal mechanisms.<sup>21</sup> Allwood *et al.* solved the relevant rate equations with approximate parameters and found that this photo/thermal ionization should be more efficient than three-photon processes.

We have performed a similar analysis for DHB, taking advantage of our improved knowledge of the appropriate physical parameters. The model considers molecules with 4 states: a neutral ground state, a first excited state ( $S_1$ ), a two-photon excited state ( $S_n$ ), and an ion ground state. The populations of these are denoted  $n_0$ ,  $n_1$ ,  $n_2$ , and  $n_i$ , respectively. The populations are taken to be normalized, so the sum of all species is unity. The rate equation for the ground state population is:

$$dn_0/dt = -A_{01}n_0 + k_{10}n_1$$

where  $A_{01}$  is the radiative pumping to the first excited state by the laser, and  $k_{10}$  is the combined fluorescence and non-radiative decay rate from the  $S_1$  to the ground state. Otherwise the rate and energy conservation equations are as in Ref. 22 Eqns. (1) and (2). Using the experimental IP for DHB and our measured deposition of excess energy by 337 nm photons, we also obtain the result that photo/thermal ionization exceeds three photon ionization in efficiency. However, the photo/thermal mechanism is far less efficient than another mechanism involving pairs of excited molecules.

From the matrix suppression effect we have proposed an alternative mechanistic possibility, that neighboring pairs (or larger aggregates) of excited matrix molecules are strongly active in generating primary MALDI ions.<sup>9</sup> Similar mechanisms have been included in the range of possibilities considered by other authors.<sup>1,2,23</sup> Such aggregates will be the object of future study in the molecular beam, but the possible relevance of such a process can be estimated by extending the model of Ref. 22. We add the following processes:

- Pooling of 2 neighboring  $S_1$  excitations to make a doubly excited molecule and a de-excited molecule. The rate constant for this is denoted  $k_{11}$ .
- Pooling of neighboring  $S_1$  and  $S_n$  excitations to give an ion and a de-excited molecule. The rate constant for this is denoted  $k_{12}$ .
- Pooling of neighboring  $S_n$  excitations to give an ion and a de-excited molecule. The rate constant for this is denoted  $k_{22}$ .

The number of pair excitations is given by probability theory, assuming 6 nearest neighbors for each matrix molecule. Since the populations are normalized, they directly represent the probabilities that any given site is in the corresponding state:

$$n_{11} = \text{the number/probability of neighboring } S_1 \text{ excited molecules} = 6n_1^2$$

$$n_{12} = \text{the number/probability of neighboring } S_1/S_n \text{ excited molecules} = 6n_1n_2$$

$$n_{22} = \text{the number/probability of neighboring } S_n \text{ excited molecules} = 6n_2^2$$

The rate equations are then modified as follows:

$$dn_0/dt = (\text{no pooling}) + k_{11}6n_1^2 + k_{12}6n_1n_2 + k_{22}6n_2^2$$

$$dn_1/dt = (\text{no pooling}) - 2k_{11}6n_1^2 - k_{12}6n_1n_2$$

$$dn_2/dt = (\text{no pooling}) + k_{11}6n_1^2 - k_{12}6n_1n_2 - 2k_{22}6n_2^2$$

$$dn_n/dt = (\text{no pooling}) + k_{11}6n_1^2 + k_{22}6n_2^2$$

The energy equation remains unchanged. These are now a set of first order non-linear differential equations, which were numerically solved using fourth order Runge–Kutta methods in double precision. Accuracy was checked by decreasing the step size until no further changes occurred. Using parameters as in Ref 22, except where data exists for DHB,

we obtained the curves in Fig. 5. The pooling rates were all set to  $10^9/s$ , slightly more than the total  $S_1$  decay rate ( $0.2 \times 10^9/s$ ). Decreasing the pooling rates to  $10^8/s$  has little effect on net ion production, radiative up-pumping is limiting. Remarkably, even at pooling rates of only  $10^6/s$  ion production is still double that of the single center model.

Clearly the pooling/thermal mechanism leads to much greater ion production than the single center process considered earlier. In both models, but particularly for the pooling case, ion production is delayed noticeably with respect to the laser pulse. This is due to energy storage in the  $S_1$  state, with its lifetime of 5 ns. Relaxation from the  $S_1$  continues to heat the sample after the peak of the laser pulse, and  $S_1-S_1$  pooling continues to generate ions even after the laser pulse is gone. While it remains to find experimental measures for the pooling parameters, the multicenter ionization model appears very plausible for DHB in UV MALDI, at this time.

## Conclusions

Molecular beam methods coupled with laser spectroscopy were used to measure MALDI-relevant properties of single 2,5-dihydroxybenzoic acid molecules in the gas phase. Fluorescence excitation (absorption) and dispersed fluorescence spectra have been measured, as well as two-color photoionization efficiency curves. The sequential two-photon ionization threshold is found at 8.05 eV, this is taken to be the ionization potential. The IP is above twice the nitrogen laser photon energy. Three-photon ionization (1+2) via the  $S_1$  intermediate state was found to be negligible. The low IP explains the lack of analyte radical cations in MALDI mass spectra using DHB as matrix, since electron transfer reactions will be unfavorable for many common analytes.

The fluorescence spectra show that no intra-molecular ESPT reaction occurs in the  $S_1$  state, despite the occurrence of this reaction in related salicylates. The reaction is also not induced by clustering with water, nor is there evidence of it in water or methanol solution. 'Classical' ESPT from DHB to analytes is thus regarded as an improbable mechanism in MALDI. In contrast, observation of HQ in MALDI plumes and  $TEA \bullet H^+$  products from  $HQ \bullet TEA^+$  clusters provides an example of alternative protonation mechanisms that could be active in MALDI with DHB matrix.

On the basis of these and earlier results, multi-center excitation models are considered the prime candidates for explaining UV MALDI. As an example, we have extended the photo/thermal ionization model of Allwood *et al.*, and found that two-center processes can be dominant over a wide range of parameters. Further work is in progress to determine the properties of DHB aggregates and other matrix molecules in the molecular beam.

## References

1. H. Ehring, M. Karas and F. Hillenkamp, *Org. Mass Spectrom.* **27**, 472 (1992).
2. P.-C. Liao and J. Allison, *J. Mass Spectrom.* **30**, 408 (1995).
3. V. Bökelmann, B. Spengler and R. Kaufmann, *Eur. Mass Spectrom.* **1**, 81 (1995).
4. M. E. Gimon, L. M. Preston, T. Soluki, M. A. White and D. H. Russell, *Org. Mass Spectrom.* **27**, 827 (1992); M. P. Chiarelli, A. G. Sharkey and D. M. Hercules, *Anal. Chem.* **65**, 307 (1993).
5. J. Krause, M. Stoeckli and U. P. Schlunegger, *Rapid Commun Mass Spectrom.* **10**, 1927 (1996).
6. A. Weller, *Z. Elektrochem.* **60**, 1144 (1956).
7. R. Knochenmuss, V. Karbach, C. Wickleder, S. Graf and S. Leutwyler, *J. Phys. Chem.* **102**, 1935 (1998).
8. R. Knochenmuss, *J. Phys. Chem.* **99**, 3881 (1995).
9. R. Knochenmuss, F. Dubois, M. J. Dale and R. Zenobi, *Rapid Commun. Mass Spectrom.* **10**, 871 (1996).
10. X. Tang, M. Sadeghi, Z. Olumee and A. Vertes, *Rapid Commun. Mass Spectrom.* **11**, 484 (1997).
11. H. Ehring and B. Sundqvist, *J. Mass Spectrom.* **31**, 1303 (1995).
12. T. W. Heise and E. S. Yeung, *Anal. Chim. Acta* **299**, 377 (1995).
13. D. A. Allwood, R. W. Dreyfus, I. K. Perera and P. E. Dyer, *Rapid Commun. Mass Spectrom.* **10**, 1575 (1996).
14. L. Sumner, Y. Huang and D. H. Russell, *Proc. 44th ASMS Conf. on Mass Spectrom.* 271 (1996).
15. M. W. Schmidt, K. K. Baldrige, J. A. Boatz, S. T. Elbert, M. S. Gordon, J. J. Jensen, S. Koseki, N. Matsunaga, K. A. Nguyen, S. Su, T. L. Windus, M. Dupuis and J. A. Montgomery, *J. Comput. Chem.* **14**, 1347 (1993).
16. S. G. Lias, J. F. Liebman, R. D. Levin and S. A. Kafafi, *NIST Standard Reference Database 19A* U.S: Dept. of Commerce, Gaithersburg (1993).
17. L. Helmbrook, J. E. Kenney, B. E. Kohler and G. W. Scott, *J. Phys. Chem.* **87**, 280 (1983); P. M. Felker, W. R. Lambert and A. H. Zewail, *J. Chem. Phys.* **77**, 1603 (1982).
18. F. Lahmani and A. Zehnacker-Rentien, *J. Phys. Chem.* **101**, 6141 (1997).
19. R. Knochenmuss, P. L. Muiño and C. Wickleder, *J. Phys. Chem.* **100**, 11 218 (1996); R.

- Knochenmuss and S. Leutwyler, *J. Chem. Phys.* **91**, 1268 (1989).
20. M. C. Land and G. R. Kinsel, *Proc. 45th ASMS Conf. on Mass Spectrom.*, 850 (1997).
21. K. Dreisewerd, M. Schürenberg, M. Karas and F. Hillenkamp, *Int. J. Mass Spectrom. Ion Processes* **141**, 127 (1995).
22. D. A. Allwood, P. E. Dyer and R. W. Dreyfus, *Rapid Commun. Mass Spectrom.* **11**, 499 (1997).
23. B. Spengler, M. Karas, U. Bahr and F. Hillenkamp, *J. Phys. Chem.* **91**, 6502 (1987); and R. E. Johnson, *Int. J. Mass Spectrom. Ion Processes* **139**, 25 (1994).



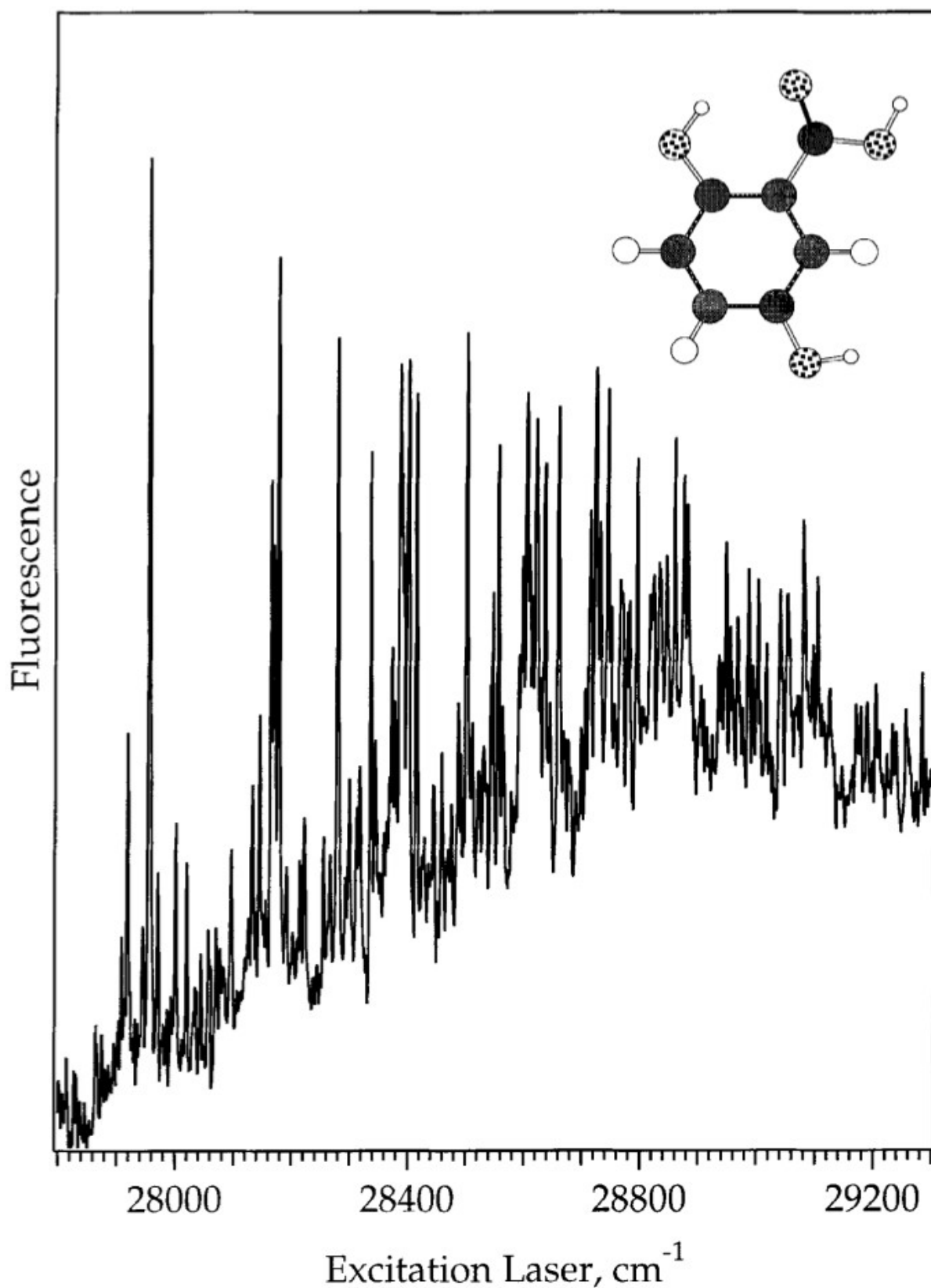


**Figure 1.** Total fluorescence excitation spectrum of jet-cooled 2,5-dihydroxybenzoic acid. The calculated minimum energy conformation is shown in the inset. The electronic origin transition is found at 27 957 cm<sup>-1</sup> (357.69 nm). The spectrum is quite congested due to many active modes which form progressions and combinations.

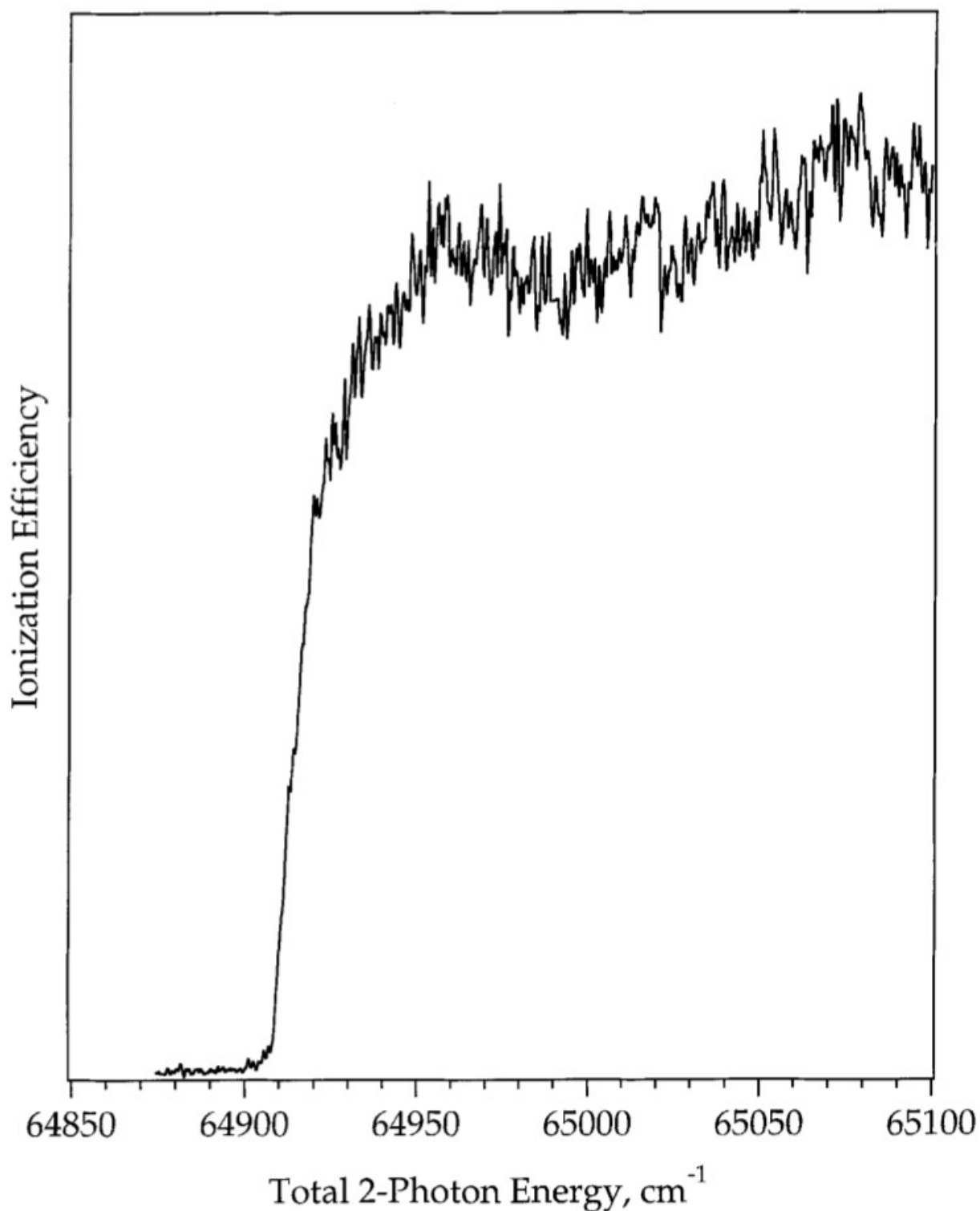


**Figure 2.** Two-color photoionization efficiency curve of jet-cooled 2,5-dihydroxybenzoic acid. The first laser was set at the  $S_1$  electronic origin, the second laser was scanned. The sharpness of the step allows accurate determination of the adiabatic ionization potential. A value of  $64\,907\text{ cm}^{-1}$ , or  $8.05\text{ eV}$  is found by extrapolation of the linear, central part of the step.

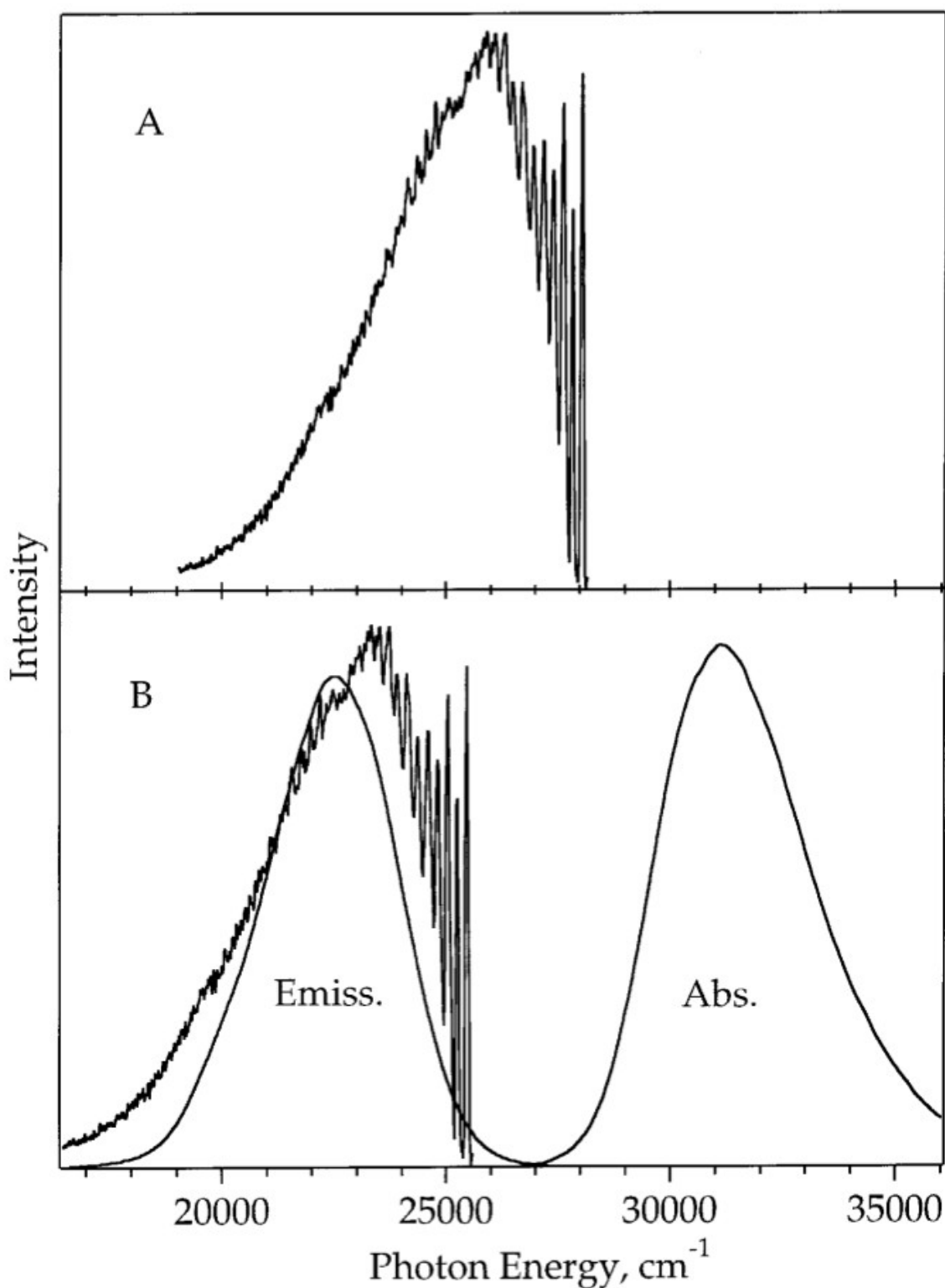


**Figure 3.** (a) Dispersed fluorescence spectrum of jet-cooled 2,5-dihydroxybenzoic acid, excited at the  $S_1$  electronic origin, which corresponds to the first band at the right of the spectrum. The spectrum begins at the excitation wavelength, and shows no anomalous red shift. The typical salicylate proton transfer emission band peaking at  $22\,000\text{ cm}^{-1}$  is also absent. (b) Comparison of solution and gas-phase spectra. The spectrum of part (a) has been shifted horizontally to compensate for solvation effects. The solution spectrum is seen to be unremarkable, showing no signs of excessive broadening or shifting.

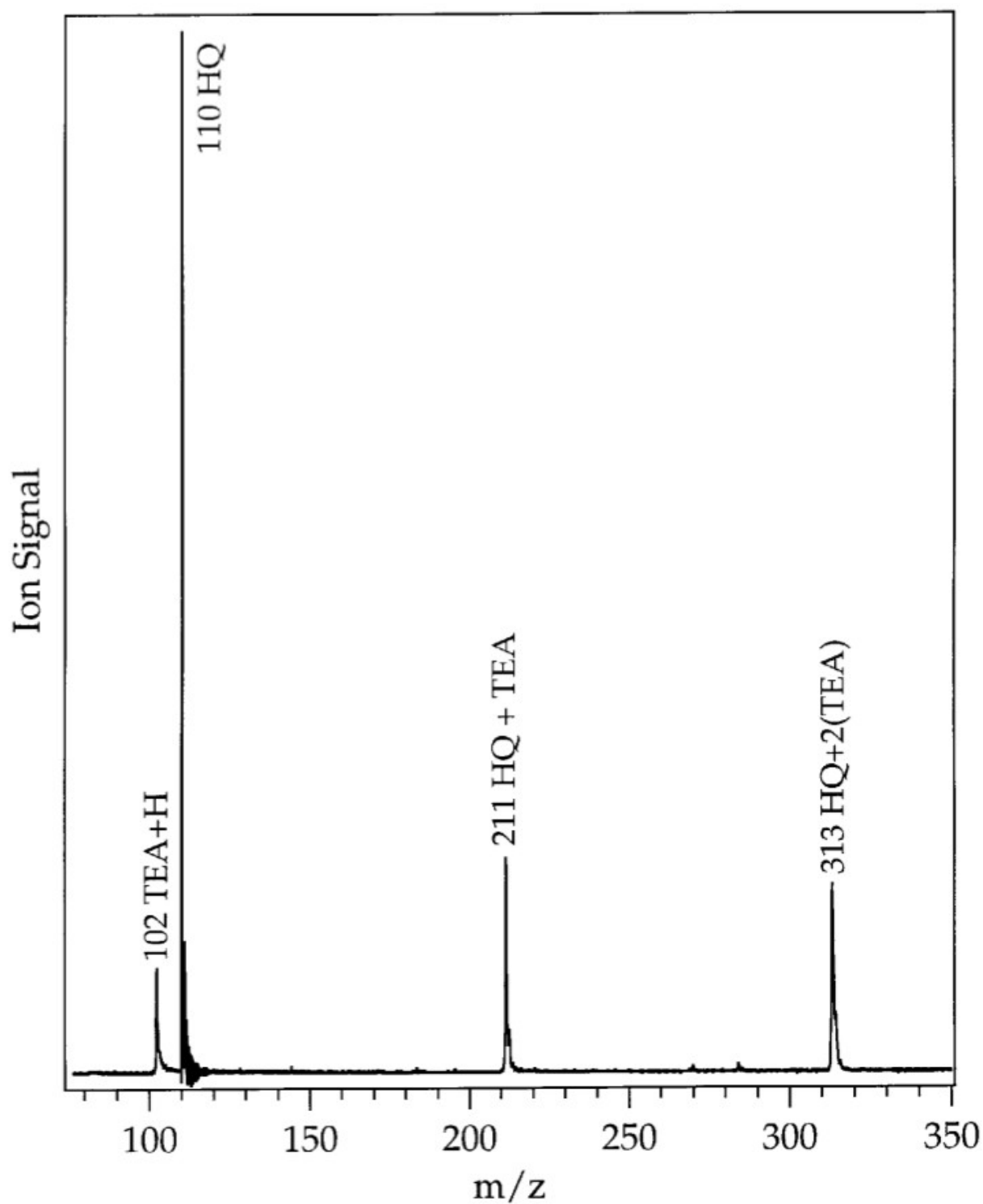


**Figure 4.** Mass spectrum of hydroquinone (HQ) clustered with triethylamine (TEA). The ionization wavelength was 270 nm. The protonated TEA signal at  $m/z$  102 was found to be strongly correlated with the  $\text{HQ}\bullet\text{TEA}^+$  cluster, but not with HQ or larger clusters.  $\text{TEA}\bullet\text{H}^+$  is therefore a fragmentation product of  $\text{HQ}\bullet\text{TEA}^+$ .

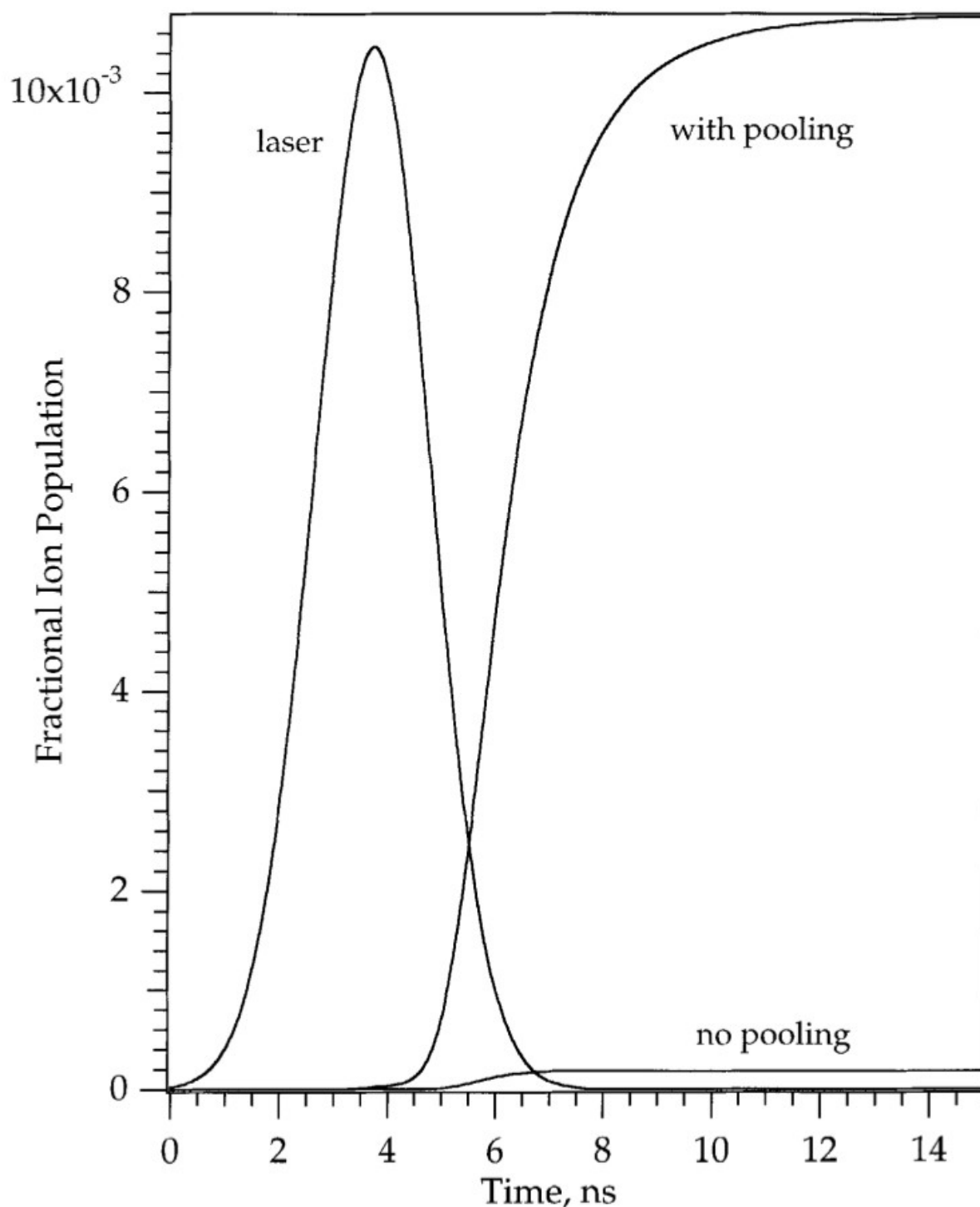


**Figure 5.** Photo/thermal ionization model with and without the two-center energy pooling process described in the text. In both cases the parameters measured here for DHB are used. The laser pulse is shown scaled to fit the graph. Constants specific to DHB were: ionization potential = 8.05 eV, energy of first excited state = 3.466 eV, excess energy after 337 nm excitation in  $S_1$  = 0.21 eV, energy gap from upper excited state to ion = 0.90 eV,  $S_1$  lifetime = 5 ns,<sup>11</sup> solid state quantum efficiency = 0.2.<sup>11</sup> The pooling rate constants were all set to  $1 \times 10^9 \text{ s}^{-1}$ .